Three dimensional magnetotelluric modelling of Vulcano Island (Eolie, Italy) and its implications for understanding recent volcanic unrest

Maria Giulia Di Giuseppe[1], Roberto Isaia[2], and Antonio Troiano[3]

[1]INGV
[2]Istituto Nazionale di Geofisica e Vulcanologia, sezione di Napoli Osservatorio Vesuviano
[3]Istituto Nazionale di Geofisica e Vulcanologia - Osservatorio Vesuviano

December 7, 2022

Abstract

Resistivity imaging obtained by a short period magnetotelluric survey identified the electrical resistivity patterns below Vulcano Island to a depth of 2 km below sea level. In the 3D resistivity model, clear contrasts generally characterized the caldera faults, whereas volcanic edifices, craters, volcanic conduits, and/or eruptive fissures corresponded to superficially high resistivity anomalies. Among the most prominent detected structures, a resistive anomaly located below La Fossa crater, which extends 2 km below the surface, likely represents a "conduit" structure, along which magmatic fluids preferably ascend. Other resistivity anomalies, mainly aligned in the N-S direction, characterized the island sector where considerable amounts of deep subsurface fluids accumulate and mix with the ascending magmas related to the most recent volcanic dynamics. The interpretation of the main features reconstructed through the magnetotelluric investigation significantly contributes to understanding the current unrest at Vulcano.

Hosted file

`essoar.10512832.1.docx` available at https://authorea.com/users/563967/articles/611008-three-dimensional-magnetotelluric-modelling-of-vulcano-island-eolie-italy-and-its-implications-for-understanding-recent-volcanic-unrest

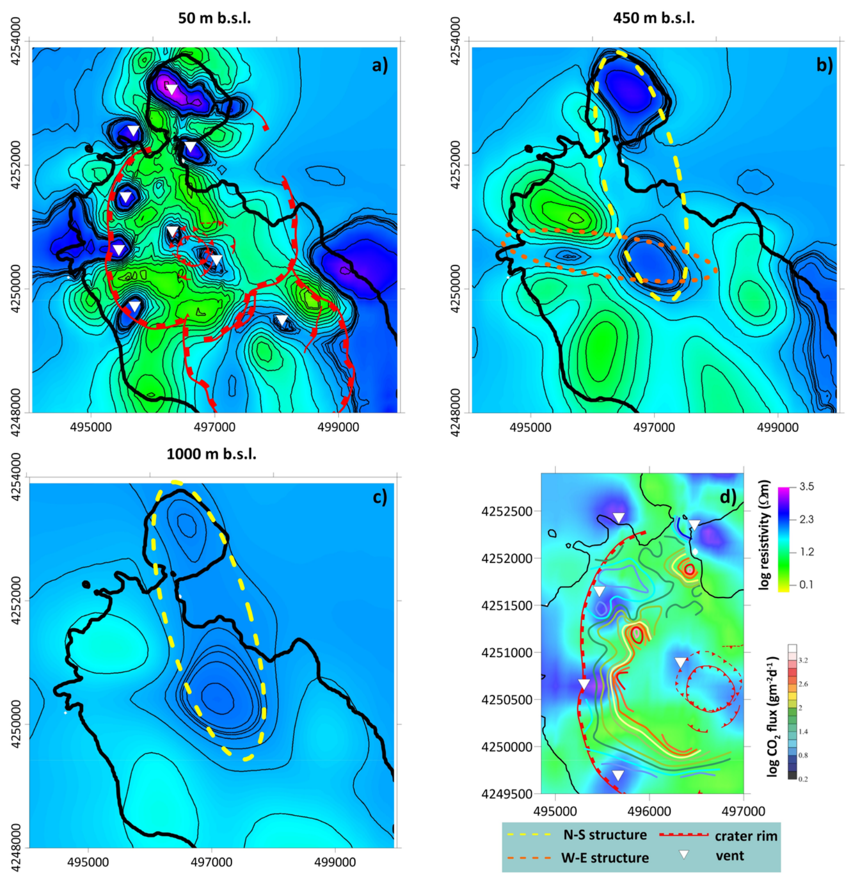
50 m b.s.l.
a)
450 m b.s.l.
b)
1000 m b.s.l.
c)
d)
log resistivity (Ωm)
log CO2 flux (gm⁻²d⁻¹)
N-S structure
W-E structure
crater rim
vent

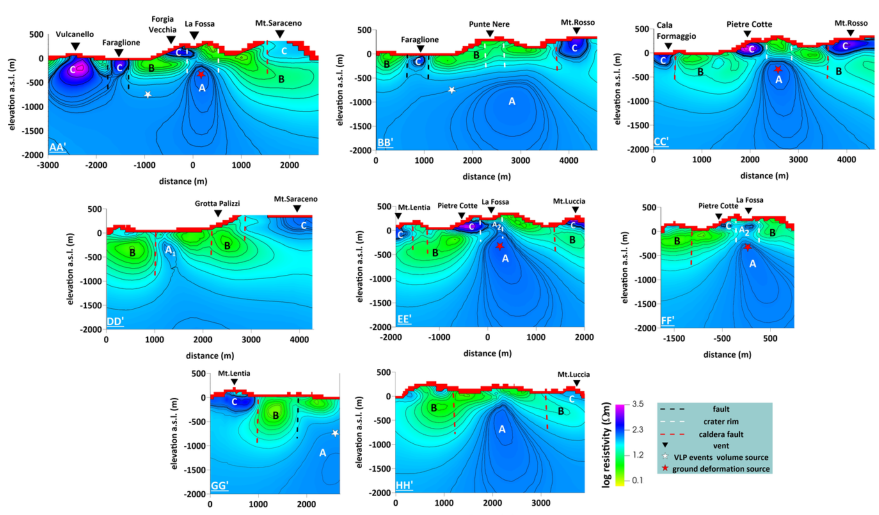
Vulcanello
Faraglione
Forgia Vecchia
La Fossa
Mt.Saraceno
Punte Nere
Mt.Rosso
Cala Formaggio
Pietre Cotte
Grotta Palizzi
Mt.Lentia
Mt.Luccia
AA'
BB'
CC'
DD'
EE'
FF'
GG'
HH'
elevation a.s.l. (m)
distance (m)
log resistivity (Ωm)
fault
crater rim
caldera fault
vent
VLP events volume source
ground deformation source

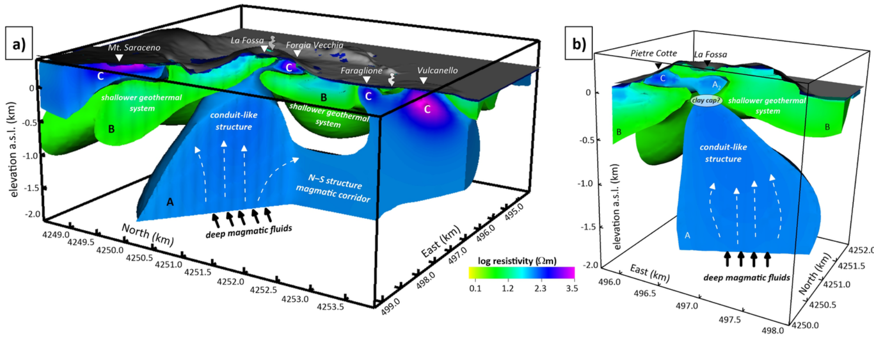
a)
Mt. Saraceno
La Fossa
Forgia Vecchia
Faraglione
Vulcanello
shallower geothermal system
conduit-like structure
N-S structure magmatic corridor
deep magmatic fluids
elevation a.s.l. (km)
North (km)
East (km)
log resistivity (Ωm)
b)
Pietre Cotte
La Fossa
clay cap
shallower geothermal system
conduit-like structure
deep magmatic fluids
elevation a.s.l. (km)
East (km)
North (km)

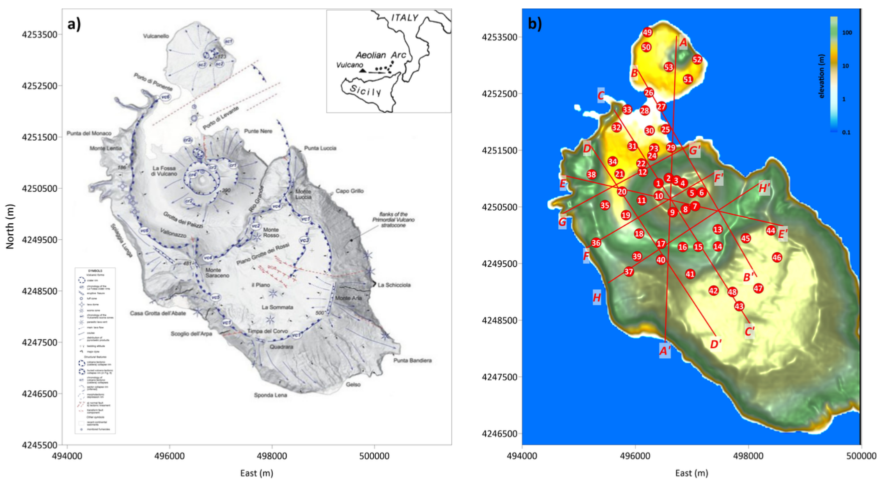
a)
ITALY
Aeolian Arc
Vulcano
Sicily
Vulcanello
La Fossa di Vulcano
Monte Saraceno
La Sommata
Il Piano
North (m)
East (m)
b)
elevation (m)
North (m)
East (m)

Three dimensional magnetotelluric modelling of Vulcano Island (Eolie, Italy) and its implications for understanding recent volcanic unrest

Maria Giulia Di Giuseppe, Roberto Isaia, Antonio Troiano

INGV-Sezione di Napoli, Osservatorio Vesuviano, Via Diocleziano 328, Napoli

Keywords

Vulcano Island; Magnetotelluric imaging; Volcanic edifices; Caldera structures

Key points

- A 3D model is presented for Vulcano Island, developed by magnetotelluric prospection that details structures down to a depth of 2 km.
- Resistivity anomalies reveal the most significant volcanic structures and features, such as conduits, faults and fractured zones.
- The complete tectonic setting of the volcano is defined, from which relevant clues about the ongoing volcanic unrest can be derived.

Abstract

Resistivity imaging obtained by a short period magnetotelluric survey identified the electrical resistivity patterns below Vulcano Island to a depth of 2 km below sea level. In the 3D resistivity model, clear contrasts generally characterized the caldera faults, whereas volcanic edifices, craters, volcanic conduits, and/or eruptive fissures corresponded to superficially high resistivity anomalies. Among the most prominent detected structures, a resistive anomaly located below La Fossa crater, which extends 2 km below the surface, likely represents a "conduit" structure, along which magmatic fluids preferably ascend. Other resistivity anomalies, mainly aligned in the N S direction, characterized the island sector where considerable amounts of deep subsurface fluids accumulate and mix with the ascending magmas related to the most recent volcanic dynamics. The interpretation of the main features reconstructed through the magnetotelluric investigation significantly contributes to understanding the current unrest at Vulcano.

Plain language summary

Vulcano is an active volcanic island located in the Aeolian archipelago that attracts touristic interest linked to volcano-related phenomena. The high exposure of inhabited areas of the island makes the volcanic risk high, even for small eruptive events, as occurred frequently in historical times. After the last eruption (1888-1890) at the La Fossa crater, unrest phases have been recorded and monitored since 1988. A new volcanic crisis, including increased fumarole temperatures, enlarged fumarolic areas, gas composition changes, ground deformation, and seismicity, have been ongoing since 2021.

Geophysical prospection activities based on the reconstruction of electrical resistivity represent a relevant task while looking for an increase in the knowledge of the volcano island volcanic system. This study presents the first three dimensional (3D) model of the structure of the La Fossa caldera down to 2 km depth, gathered through a new magnetotelluric prospecting. This survey provides original information on the main structure of the caldera and the related subsurface fluid circulation. Furthermore, the volcanological interpretation of such findings also furnishes relevant clues about the causes of the geophysical and geochemical anomalies detected in the last year, which involved the Vulcano shallow hydrothermal system, highlighting the potential for possible hydrothermal/phreatic eruptive events.

1. Introduction

The island of Vulcano is the southernmost subaerially exposed volcanic edifice of the Aeolian archipelago. Vulcano has been responsible for many eruptions throughout history, including at least three phreatic eruptions (Arrighi et al., 2006; De Astis et al., 2013, 2003; Dellino et al., 2011; Di Traglia et al., 2013; Frazzetta et al., 1983; Fusillo et al., 2015; Gioncada and Sbrana, 1991; Gurioli et al., 2012; Keller, 1980; Peccerillo et al., 2006; Rosi et al., 2018). Considering the tourism value offered by volcano-related phenomena (e.g., hot mud flows and fumaroles) and the high exposure of the local inhabited areas to volcanic activity, the volcanic risks on the island are quite high, even for small eruption events. The most recent eruption on the island occurred between 1888 and 1890 AD, and since then, Vulcano's hydrothermal system has been the site of different volcanic unrest (Alparone et al., 2019, 2010; Capasso et al., 1999; Chiodini et al., 1995; Diliberto et al., 2002; Inguaggiato et al., 2022; Paonita et al., 2013). In particular, in 2021, the routinely monitored geochemical and geophysical parameters showed significant changes, suggesting a potential increase of magmatic fluids within the shallow geothermal system. Such fluctuations involved changes to the isotopic composition of the volcanic gases (a well-known magmatic tracer), temperature changes at both the crater and in groundwater in the fumaroles, the opening of new fumarolic vents, and changes to the rate of soil gas emissions observed at both the crater rim and the foot of the cone. Moreover, GPS data revealed an expansion of the crater zone (confirmed by InSAR data and geodetic surveys), which was traced to a pressurized source at approximately 350 m depth below sea level (b.s.l.) (Paonita et al., 2022). The occurrence of very long period (VLP) seismicity, centred northwards of the Vulcano crater (named the 'La Fossa' cone) at an average depth of 750 m b.s.l., has been associated with plausible fluid migration (Gangemi et al., 2022). The subsequent rise in the Vulcano alert level, which was elevated from green to yellow, has led to increased scientific attention in the region. Prospection activities concerning the island and the volcano-tectonic characterization of its structures, including the relation between the volcano and the geothermal system, represent one of the primary research topics at this time.

In similar contexts, prospections based on electrical resistivity measurements have already been shown to be adequate tools for studying deep buried structures (Brothelande et al., 2014; Di Giuseppe et al., 2017, 2015; Finizola et al., 2004; Hogg et al., 2018; Pous et al., 2002; Seki et al., 2021, 2016; Soueid Ahmed et al., 2018; Troiano et al., 2021, 2019, 2014, 2008; Tsukamoto et al., 2018). Furthermore, electrical resistivity has previously been used on same Vulcano Island (Barde-Cabusson et al., 2009; Revil et al., 2010, 2008). Through the study of this physical parameter, which is highly sensitive to temperature, porosity, permeability, and the presence of fluids (Barde-Cabusson et al., 2013; Brothelande et al., 2014; Di Giuseppe and Troiano, 2019; Gresse et al., 2018, 2017; Unsworth and Rondenay, 2013), it is possible to evaluate the degree of fluid permeation in buried rock volumes and to reconstruct the subsurface structural characteristics (e.g., faults, fractures, and lithologies) that coexist in active volcanic environments. Considering that the deep structures beneath the La Fossa caldera remain undefined at present (Chiarabba et al., 2004; De Ritis et al., 2005), the mapping of the local subsurface structures by electrical resistivity presents a great opportunity to increase the available knowledge regarding volcanic island systems. The purpose of this study is to present the first three dimensional electrical resistivity model of the subsurface structure of the La Fossa caldera down to a depth of 2 km obtained by magnetotelluric (MT) prospection. This survey provides original information regarding the main structure of the caldera and the related subsurface fluid circulation. Furthermore, the volcanological interpretation of such findings also provides relevant clues about the causes of the abovementioned geophysical and geochemical anomalies detected over the last year; anomalies that involved the shallow hydrothermal system below the island and may indicate the potential for possible hydrothermal/phreatic events.

2. Volcanological Framework

The island of Vulcano is the exposed summit of an active NW–SE-elongated composite volcano located in the southernmost sector of the Aeolian archipelago (Vilardo et al., 2013). It is nearly connected with the nearby Lipari complex, from which it is separated only by a shallow water saddle at depths of approximately 50 m b.s.l. (De Astis et al., 2013). Volcanism spread across eight eruptive epochs separated by volcano-tectonic events that produced two intersecting multistage calderas and major quiescent intervals (De Astis et al., 2013). Vulcano rocks range from basalt to rhyolite and show variable alkali contents, that roughly increase over time, according to the structural and volcanological evolution of the volcanic system. The locations of the volcanic centres at Vulcano and Lipari islands have been largely controlled by normal faults (mainly striking NNW SSE and N S) that were particularly dominated over the last approximately 55 ka and by N S structures during the most recent periods of volcanic activity (8 ka and <2 ka; Ruch et al., 2016). The most recent volcanic period produced eruptions ranging from Strombolian and effusive types to Vulcanian eruptive cycles, and included a few significant phreatomagmatic eruptions (Selva et al., 2020 and references therein), with somewhat simultaneous activity located within La Fossa Caldera and the Vulcanello vent (e.g., Fusillo et al., 2015). The large phreatic explosions from the La Fossa crater that involved the hydrothermal system produced extensive eruption-like phenomena, including convective columns, ballistic ejection, and pyroclastic density currents, and have been reconstructed by stratigraphic records (such as the Breccia di Commenda event; (Di Traglia et al., 2013; Frazzetta et al., 1983; Rosi et al., 2018; Selva et al., 2020).

After the last eruption (1888-1890) at the La Fossa crater, a continuous gas discharge developed in the two main fumarolic fields (one on the active crater rim and the other near the Levante shore). In addition, widespread diffuse degassing through the soil, both on the crater rim and at a few sites on the caldera floor, also occurred. Unrest phases, including increased fumarole temperature, enlarged fumarolic areas, changes in gas composition, ground deformation, and seismicity, have been recorded and monitored since 1988.

The ongoing unrest showed a sharp increase in degassing activity, both from the crater fumaroles and through the soil, including a drastic increase in both the magmatic component of the fumarole composition and the temperature. Local seismicity (VLP events) and ground deformation phenomena centred below the northern sector of La Fossa crater have also been recorded by the monitoring system maintained by the Istituto Nazionale Geofisica e Vulcanologia (INGV) since August-September 2021 (INGV, 2022). The recorded anomalies are still evident, with the greatest increase in hydrothermal activity observed in Baia di Levante, where abrupt outgassing episodes have led the municipality to prohibit access to portions of the beach.

3. MT Investigations

Figure 1b shows the locations of the 53 sites where fieldwork and MT data collection were conducted. Measurements were collected by a Stratagem EH4 instrument produced by Geometrics Measurements, which equipped with additional low frequency magnetometers and electric dipoles to acquire signals in the [10^{-1}-10^{5}] Hz frequency band. A controlled source was used in the frequency range from 1,000 Hz to 64,000 Hz.

Preliminary analyses of the acquired data focussed on data dimensionality, which was estimated through the study of the Phase Tensor (Caldwell et al., 2004; Figs. S1, S2) and via the analysis of the influence of the Vulcano ground-level topography and seafloor bathymetry on the MT dataset (Yang et al., 2010; S3). As a consequence of such analyses, the inversion of the Vulcano MT dataset was done by adopting the 3D code ”Modular system for Electromagnetic inversion” (ModEM) (Egbert and Kelbert, 2012; Kelbert et al., 2014; Meqbel, 2009), which is currently considered something of a standard for similar analyses. For detail on the model mesh adopted during the inversion see the Supplementary Information.

The input data were decimated to 8 logarithmically spaced frequencies, ranging from 1000 to 0.31 Hz. A fixed error floor equal to 5% was applied on the nondiagonal elements of the impedance tensor, which were the solely modes inverted due to the indications obtained by the data preliminar analyses. For the final inversion model, it took 73 interactions for the ModEM inversion code to converge at a 1.98 value for the normalized root mean square (nRMS: Fig. S4). Fig. S5 shows a comparison between the measured and predicted data for all sites and frequencies.

4. The 3D Electrical Resistivity Model

The 3D MT image of the central-northern sector of Vulcano allowed for the identification of the subsurface electrical resistivity patterns down to a depth of 2 km b.s.l. Several resistivity anomalies appeared in the 3D model concerning the volcano's different structures or physical conditions, which can be seen by examining the several 2D slices sketched in Figure 2, which refer to the traces along the profiles shown in Figure 1b (red lines), and the horizontal maps sketched in Figure 3 (each one pertaining to a different elevation).

These sections and maps revealed many relevant resistivity anomalies, labelled with capital letters in Figure 2. The most significant among these features is the resistivity anomaly on the order of hundreds of Ω m, labelled with A in the maps and sections, whose location closely corresponds with the La Fossa crater. This feature has a cylindrical symmetry at the top section and increases in size from approximately 500 m b.s.l. As shown in Figure 2 (section AA'), the top of the A anomaly rises to approximately 200-300 m below the La Fossa crater and extends to a depth of 600 m to the north and 1000 m to the south of the crater. On the other hand, west of the crater, the top of the A structure lies at a depth of approximately 1000 m, whereas to the east, it lies at approximately 600 m depth (Figure 2; FF' section). Finally, this anomaly also presents a small apophysis (labelled A_1), which is primarily evident in section DD'. The apical part of structure A also appears to be connected to a further, more superficial, anomaly of similar resistivity value, indicated by A_2. The location of this feature corresponds with the uppermost part of the La Fossa cone, which is primarily evident in sections EE' and FF'.

A low resistivity layer, denoted as B in the sections of Figure 2, is detected around structure A, and is characterized by an average value of a few tens of Ω m. This anomaly surrounds the top of the A structure and is generally confined above approximately 500 m b.s.l. to the east of the crater, though it extends to a depth of approximately 1000 m towards the west (Figure 2; sections DD', EE', GG', HH').

Several resistive anomalies of several hundred Ω m (denoted by C) interrupt the horizontal continuity of conductive layer A. However, as shown in Figure 3a (resistivity maps for elevations ranging from 50 to 450 m), these resistivity anomalies appear superficial and are confined to the first 500 m b.s.l., except those localized in the vicinity of Vulcanello.

4. Discussion/Results Interpretation

The geometry of the resistivity anomalies sufficiently highlights the different volcano-tectonic lineaments that have characterized the volcanic evolution of the island of Vulcano. Furthermore, these results provide valuable indications for understanding the interaction between the lithostratigraphic setting, fluid circulation, and the current dynamics recorded on the island. All the resistivity sections presented in Figure 2 intersect and clearly show the La Fossa caldera border structures in their different sectors, except for the submerged portion outside the area of investigation (Figure 3).

Apparent resistivity contrasts generally characterized the structures interpreted as caldera faults (Figure 2; red dotted lines) at the base of the outcropping escarpments identified as the exposed slopes of caldera collapse. Such resistivity contrasts remain evident with geologic structural data regardless of the age of the volcano-tectonic collapses reconstructed (De Astis et al., 2013). In particular, the correlation of fault scarp and resistivity contrast seems more evident in the southern sector, corresponding to the older collapse phase VC2-VC4, perhaps related to probable reactivations of these structures. In contrast, in the northwestern sector, the resistivity contrast seems to be more internal than at the morphological edge.

The calderic borders are also evident in the resistivity maps (Figure 3), where the N S aligned high resistivity anomalies are associated with the western La Fossa caldera structure (phase V6; De Astis et al., 2013).

Moreover, the resistivity sections (Figure 2) show that the highest resistivity bodies detected along the surface mainly correspond to a series of volcanic edifices, craters, volcanic conduits, and/or eruptive fissures. In addition to the domes from the Monte Lentia Formation (sections EE' and GG'), the anomalies associated with Monte Saraceno (sections DD' and AA'), Monte Rosso (sections BB' and CC'), Monte Luccia (section EE'), Cala del Formaggio (section CC') and Vulcanello (section AA') are all located along the edges of the caldera. The crater areas of La Fossa, Forgia Vecchia, Pietre Cotte, the Faraglione Tuff cone and Vulcanello are all aligned within the caldera along a N S direction (section AA'). A further resistivity anomaly in the crater summit area (indicated A_2 in sections EE' and FF') likely relates to the N S trending structure.

Resistivity maps in the first 50 m b.s.l. also allowed for a suitable identification of the previously described high resistivity bodies. Below 450 m, two resistivity anomalies that trend E W and N S are evident, the latter of which remains visible to depths in excess of 1,000 m b.s.l. (Figure 3). The E W structure corresponds to the alignment of the Lentia-La Fossa eruptive centres (Figure 3b; orange dotted line), whereas the N S structure (Figure 3b, c; yellow dotted line) sufficiently describes the alignment of the most recent historical volcanic vents on the island (Vulcanello, Faraglione, La Forgia Vecchia, and La Fossa) as well as the most active presently outgassing structures.

The primary alignment found by MT investigations along the N S direction finds strong support in the literature. Several authors (De Astis et al., 2003; Ventura et al., 1999) hypothesize that the position of surface magmatic reservoirs responsible for volcanism at Vulcano could be controlled by N S secondary faults that play a predominant role in magma upwelling in most superficial layers (<0.5

km depth; Chiarabba et al., 2004). Ruch et al., 2016 suggested that recent volcano tectonics in the islands of Lipari and Vulcano acted exclusively along a N S-directed magmatic corridor that was originally 2 km wide but thinned to 1 km over the last 2 ka. This is in relation to a constant E W-directed extensional regime and in agreement also with the geochemical petrological data which supports the existence of a single stable subsurface magmatic source oriented in a N S direction (Davì et al., 2009).

Concerning the anomalies described in the previous section, the A structure appears centred beneath the La Fossa crater. Its signature (in terms of geometry and resistivity) suggests the possible presence of a fluid permeated conduit. Through such a conduit, deeply stored magma-derived fluids could upwell towards the summit of the crater. Notably, the location and depth of the recently recorded ground deformation source at Vulcano (Paonita et al., 2022) coincide with the apical part of this resistive A-body (Figure 2; white star; sections AA', CC', EE', FF').

The conductive B anomalies could correspond with zones of higher permeability. These are indicative of the more fractured sectors close to the volcano-tectonic lineaments (Figure 2; sections AA', BB', CC', GG') and in the eastern and southernmost superficial sectors of the La Fossa cone, where rising gases in the conduit probably interact with the seawater along the main caldera and crater structures (Figure 2; sections CC', FF', HH'). The conductive environment appears generally confined to the upper 500 m and is probably the expression of the shallow hydrothermal system of the island. At those depths, there is an interface with a moderately resistive environment, which deepens only in the western intracalderic sector. There is evidence in that region of a conductivity anomaly that extends to approximately 1000 m b.s.l., which is an area close to the marginal caldera faults. These results could indicate a zone of increased fracturing and permeability that would favour deep marine ingression.

The depth of the conductive-resistive interface in the caldera can be compared with the observations made during the drilling of the Vulcano Porto deep well (Agip Report, 1987), when a transition was detected at a depth of approximately 600 m b.s.l. Corresponding to such a transition, a contrast has been reconstructed between a shallower sector that consists of more permeable rocks with a low geothermal gradient, convective regime, and a deeper sector characterized by more impermeable lavas with a high geothermal gradient, high temperatures and a conductive regime (Agip Report, 1987). It is worth noting, however, that the conductive-resistive separation horizon detected in the N E sector of the La Fossa well also matches the source volume location of the VLP seismic event (Gangemi et al., 2022)modelled at an average depth of 750 m b.s.l. (white star in Figure 2; sections AA', BB', FF, GG').

In addition, the areal distribution map of surface CO2 fluxes (INGV, 2022) shows a good correlation between the main degassing structures and the electrical anomalies detected by the resistivity images. In particular, the anomalous Grotta dei Palizzi zone, as well as that of the Sicilia campsite, is located in the sector affected by the resistivity contrasts that highlight the La Fossa caldera marginal faults. Additionally, the Baia di Levante area is located along the N S structure and probably intersects with NE SW faults. Comparing the surface resistivity maps (z=50 m b.s.l.) and the CO_2 flow anomalies (INGV, 2022), , shows that CO_2 flow is confined to the inner edge of the higher resistivity bodies (Figure 3d). This confirms that the maximum expression of ground/soil degassing occurred along the main structures already highlighted in the sections of Figure 2.

Concluding Remarks and Implications

The 3D resistivity model from Vulcano describes all the island's main structures, clarifies their geometries and highlights their relationship with the most significant volcano-tectonic alignments. Additionally, these features present evidence of the eruptive history and present condition of the volcano.

The main characteristics of the 3D resistivity model, which were summarized in Figure 4, give rise to a few relevant considerations:

- Below the La Fossa main crater, the MT image detected the presence of a relatively highly resistive body (the A anomaly in Figure 2, 4), which extends down to a depth in excess of 2 km (e.g., below the maximum depth investigated by the present survey). This likely represents a conduit-like structure that acts as a preferential pathway for deep fluids of magmatic origin to move towards the surface.

- In the crater zone, the top of this conduit corresponds to the location indicated by ground deformation data modelling as the source of the ongoing volcanic unrest, which involves the Vulcano hydrothermal system. As the top of the A anomaly deepens, it moves away from the centre of the La Fossa crater. In particular, the northeastern part of the features overlaps with the source of the VLP seismic events recorded in the last year. This observation seems to correspond to the boundary between the rising magma channel and the shallower Vulcano geothermal system, in which the resistivity results show resistive and conductive behaviour, respectively.

- A series of resistivity anomalies, indicated with C in Figures 2, 4 and 4, align mainly along the N S direction and overlap with the La Forgia Vecchia and Baia di Levante degassing structure of the N NE crater sector. Such structures likely represent the region of the island where most deep-rising fluids accumulate and mix with the magmas related to the most recent volcanic activity (Figure 3d).

As a further remark, we recall the direct coupling between the top of the A anomaly and the apical A_2 anomaly, which appear to have comparable resistivity (Figure 2; Sections EE', FF'). Many studies have been done concerning MT investigations within active volcanic systems worldwide (Di Paolo et al., 2020; Gresse et al., 2021). In a good number of these cases, the studies underline the possible presence of hydrothermally altered rock volumes acting as 'clay caps' at the top of volcanic conduits (Fulignati et al., 1998), whose formation has been promoted by an intense circulation of hot fluids. Clays and hydrothermally altered rocks have very high conductivity signatures under wet conditions. However, they could present a different signature if placed in a dry environment. Regarding the A-A_2 coupling detected in the La Fossa crater case, which consists of two similarly resistive structures, we suggest the presence of a rock volume from which fluids were drained, likely due to the effects of a pressure gradient caused by a deep fluid input source that pressurized the shallower part of the La Fossa hydrothermal system. Such fluids, interacting with the surrounding rock volumes, altered the thermodynamic conditions of the hydrothermal system. This likely caused an increase in the fluid pressure, changes in fluid circulation and possible water vaporisation. This likely altered the surficial fluid circulation in the shallow system, including the water table, and led to diffuse degassing at the ground and fumaroles vent, as detected by the monitoring system.

Acknowledgments

We warmly thank the INGV colleagues Emilio Cuoco, Marco Manni, Lucia Nardone, Lucia Pruiti and Alessandro Santi for the help in the fieldwork activities. This research has been planned and supported in the framework of the INGV activities for the 2021-2022 hydrothermal crises at Vulcano.

Figure Captions

Figure 1. MT soundings carried out on the island of Vulcano. a) Morphostructural sketch map of Vulcano; b) locations of the 53 MT sites and traces of the resistivity profiles extracted by the model

Figure 2. Resistivity sections related to the profiles shown with red lines on the Vulcan map of Fig. 1b. The contour of electrical resistivity as a function of depth is represented using the reported color bar scale; symbols are represented in legend; letters are explained in the text.

Figure 3. Horizontal sections of electrical resistivity related to elevations z=50 m, z=450 m, z=1000 m a.s.l. The map shows: a) the main volcano-tectonic structures extrapolated from De Astis et al., (2013) and the eruptive centers inferred from the resistivity anomalies; b) and c) the areas characterized by E-W (dashed orange line) and N-S (dashed yellow line) trending structures highlighted by the resistivity anomalies; d) Curves extracted from the spatial distribution of CO2 fluxes emitted to the ground (INGV Bulletin) superimposed on a map (z=50 m a.s.l.) of 3D electrical resistivity model.

Figure 4. Sketch model of the La Fossa caldera deducted by the 3D resistivity model obtained through the current MT survey. Interpretative elements are also superimposed on the model. In particular, 4a shows a visualization (view from the east) showing the depth trend of the most resistive bodies aligned in the N-S direction; 4b shows the detected anomalies along an E-W alignement

(view from the south). The common logarithmic scale represents the electrical resistivity.

Author contributions

M.G.D.G., R.I and A.T. equally contributed to the geophysical application, from field operations to data processing and inversion to the text and the final interpretation.

Open Research

All data generated or analysed during this study are included in this published article [and its supplementary information files]. Following the project data policies, the data will be available and registered in the INGV database "Geoelectric tomographic maps", INGV Data Management Office (2020). INGV Open Data Registry, the metadata catalogue of the Istituto Nazionale di Geofisica e Vulcanologia. Istituto Nazionale di Geofisica e Vulcanologia (INGV). https://doi.org/10.13127/data-registry.

Competing interest

The authors declare that they have no competing interests.

References

Agip Report, 1987. Joint Venture AGIP-EMS-ENEL, Permesso di ricerca" Vulcano" sintesi geomineraria finale. AGIP Internal Report.Alparone, S., Bonforte, A., Gambino, S., Guglielmino, F., Obrizzo, F., Velardita, R., 2019. Dynamics of Vulcano Island (Tyrrhenian Sea, Italy) investigated by long-term (40 years) geophysical data. Earth-Science Reviews 190, 521–535. https://doi.org/10.1016/j.earscirev.2019.01.002Alparone, S., Cannata, A., Gambino, S., Gresta, S., Milluzzo, V., Montalto, P., 2010. Time-space variation of volcano-seismic events at La Fossa (Vulcano, Aeolian Islands, Italy): new insights into seismic sources in a hydrothermal system. Bull Volcanol 72, 803–816. https://doi.org/10.1007/s00445-010-0367-6Arrighi, S., Tanguy, J.-C., Rosi, M., 2006. Eruptions of the last 2200 years at Vulcano and Vulcanello (Aeolian Islands, Italy) dated by high-accuracy archeomagnetism. Physics of the Earth and Planetary Interiors 159, 225–233. https://doi.org/10.1016/j.pepi.2006.07.010Barde-Cabusson, S., Bolós, X., Pedrazzi, D., Lovera, R., Serra, G., Martí, J., Casas, A., 2013. Electrical resistivity tomography revealing the internal structure of monogenetic volcanoes. Geophysical Research Letters. https://doi.org/10.1002/grl.50538Barde-Cabusson, S., Finizola, A., Revil, A., Ricci, T., Piscitelli, S., Rizzo, E., Angeletti, B., Balasco, M., Bennati, L., Byrdina, S., Carzaniga, N., Crespy, A., Di Gangi, F., Morin, J., Perrone, A., Rossi, M., Roulleau, E., Suski, B., Villeneuve, N., 2009. New geological insights and structural control on fluid circulation in La Fossa cone (Vulcano, Aeolian Islands, Italy). Journal of Volcanology and Geothermal Research 185, 231–245. https://doi.org/10.1016/j.jvolgeores.2009.06.002Brothelande, E., Finizola, A., Peltier, A., Delcher, E., Komorowski, J.C., Di Gangi, F., Borgogno, G., Passarella, M., Trovato, C., Legendre, Y., 2014. Fluid circulation pattern inside La Soufrière volcano (Guadeloupe) inferred from combined electrical resistivity tomography, self-potential, soil temperature and diffuse degassing measurements. Journal of Volcanology and Geothermal Research 288, 105–122. https://doi.org/10.1016/j.jvolgeores.2014.10.007Caldwell, T.G., Bibby, H.M., Brown, C., 2004. The magnetotelluric phase tensor. Geophysical Journal International 158, 457–469. https://doi.org/10.1111/j.1365-246X.2004.02281.xCapasso, G., Favara, R., Francofonte, S., Inguaggiato, S., 1999. Chemical and isotopic variations in fumarolic discharge and thermal waters at Vulcano Island (Aeolian Islands, Italy) during 1996: evidence of resumed volcanic activity. Journal of Volcanology and Geothermal Research 88, 167–175. https://doi.org/10.1016/S0377-0273(98)00111-5Chiarabba, C., Pino, N.A., Ventura, G., Vilardo, G., 2004. Structural features of the shallow plumbing system of Vulcano Island Italy. Bull Volcanol 66, 477–484. https://doi.org/10.1007/s00445-003-0331-9Chiodini, G., Cioni, R., Marini, L., Panichi, C., 1995. Origin of the fumarolic fluids of Vulcano Island, Italy and implications for volcanic surveillance. Bull Volcanol 57, 99–110. https://doi.org/10.1007/BF00301400Davì, M., Behrens, H., Vetere, F., De Rosa, R., 2009. The viscosity of latitic melts from Lipari (Aeolian Islands, Italy): Inference on mixing–mingling processes in magmas. Chemical Geology 259, 89–97. https://doi.org/10.1016/j.chemgeo.2008.10.009De Astis, G., Lucchi, F., Dellino, P., La Volpe, L., Tranne, C.A., Frezzotti, M.L., Peccerillo, A., 2013. Chapter 11 Geology, volcanic history and petrology of Vulcano (central Aeolian archipelago). Memoirs 37, 281–349. https://doi.org/10.1144/M37.11De Astis, G., Ventura, G., Vilardo, G., 2003. Geodynamic significance of the Aeolian volcanism (Southern Tyrrhenian Sea, Italy) in light of structural, seismological, and geochemical data: GEODYNAMICS OF THE AEOLIAN VOLCANISM. Tectonics 22, n/a-n/a. https://doi.org/10.1029/2003TC001506De Ritis, R., Blanco-Montenegro, I., Ventura, G., Chiappini, M., 2005. Aeromagnetic data provide new insights on the volcanism and tectonics of Vulcano Island and offshore areas (southern Tyrrhenian Sea, Italy). Geophysical Research Letters 32. https://doi.org/10.1029/2005GL023465Dellino, P., De Astis, G., La Volpe, L., Mele, D., Sulpizio, R., 2011. Quantitative hazard assessment of phreatomagmatic eruptions at Vulcano (Aeolian Islands, Southern Italy) as obtained by combining stratigraphy, event statistics and physical modelling. Journal of Volcanology and Geothermal Research, From maars to scoria cones: the enigma of monogenetic volcanic fields 201, 364–384. https://doi.org/10.1016/j.jvolgeores.2010.06.009Di Giuseppe, M.G., Troiano, A., Di Vito, M.A., Somma, R., Matano, F., 2017. Definition of small-scale volcanic structures by electrical resistivity tomography: The Trentaremi cone, an example from the Campi Flegrei Caldera (Italy). Annals of Geophysics 60. https://doi.org/10.4401/ag-7397Di Giuseppe, M.G., Troiano, A., Fedele, A., Caputo, T., Patella, D., Troise, C., De Natale, G., 2015. Electrical resistivity tomography imaging of the near-surface structure of the Solfatara crater, Campi Flegrei (Naples, Italy). Bulletin of Volcanology 77. https://doi.org/10.1007/s00445-015-0910-6Di Giuseppe, M.G.G., Troiano, A., 2019. Monitoring active fumaroles through time-lapse electrical resistivity tomograms: an application to the Pisciarelli fumarolic field (Campi Flegrei, Italy). Journal of Volcanology and Geothermal Research 375, 32–42. https://doi.org/10.1016/j.jvolgeores.2019.03.009Di Paolo, F., Ledo, J., Ślęzak, K., Martínez van Dorth, D., Cabrera-Pérez, I., Pérez, N.M., 2020. La Palma island (Spain) geothermal system revealed by 3D magnetotelluric data inversion. Sci Rep 10, 18181. https://doi.org/10.1038/s41598-020-75001-zDi Traglia, F., Pistolesi, M., Rosi, M., Bonadonna, C., Fusillo, R., Roverato, M., 2013. Growth and erosion: The volcanic geology and morphological evolution of La Fossa (Island of Vulcano, Southern Italy) in the last 1000years. Geomorphology 194, 94–107. https://doi.org/10.1016/j.geomorph.2013.04.018Diliberto, I., Gurrieri, S., Valenza, M., 2002. Relationships between diffuse CO2 emissions and volcanic activity on the island of Vulcano (Aeolian Islands, Italy) during the period 1984–1994. Bull Volcanol 64, 219–228. https://doi.org/10.1007/s00445-001-0198-6Egbert, G.D., Kelbert, A., 2012. Computational recipes for electromagnetic inverse problems: Computational recipes for EM inverse problems. Geophysical Journal International 189, 251–267. https://doi.org/10.1111/j.1365-246X.2011.05347.xFinizola, A., Lénat, J.-F., Macedo, O., Ramos, D., Thouret, J.-C., Sortino, F., 2004. Fluid circulation and structural discontinuities inside Misti volcano (Peru) inferred from self-potential measurements. Journal of Volcanology and Geothermal Research 135, 343–360. https://doi.org/10.1016/j.jvolgeores.2004.03.009Frazzetta, G., La Volpe, L., Sheridan, M.F., 1983. Evolution of the Fossa Cone, Vulcano. Journal of Volcanology and Geothermal Research, Explosive Volcanism 17, 329–360. https://doi.org/10.1016/0377-0273(83)90075-6Fulignati, P., Gioncada, A., Sbrana, A., 1998. Geologic model of the magmatichydrothermal system of vulcano (Aeolian Islands, Italy). Mineralogy and Petrology 62, 195–222. https://doi.org/10.1007/BF01178029Fusillo, R., Di Traglia, F., Gioncada, A., Pistolesi, M., Wallace, P.J., Rosi, M., 2015. Deciphering post-caldera volcanism: insight into the Vulcanello (Island of Vulcano, Southern Italy) eruptive activity based on geological and petrological constraints. Bull Volcanol 77, 76. https://doi.org/10.1007/s00445-015-0963-6Gangemi, M.V., Alparone, S.C., Cannata, A., Di Grazia, M., 2022. Analysis of seismic signals accompaignying the unrest of Vulcano in 2021., in: Abstract Volume 5° Conferenza A. RITTMANN, 1340. Presented at the Conferenza A. Rittmann, O. Cocina, C. Tranne, A. Vona, M. Viccaro.Gioncada, A., Sbrana, A., 1991. “La Fossa caldera”, Vulcano: inferences from deep drillings. Acta Vulcanol. 115–126.Gresse, M., Uyeshima, M., Koyama, T., Hase, H., Aizawa, K., Yamaya, Y., Morita, Y., Weller, D., Rung-Arunwan, T., Kaneko, T., Sasai, Y., Zlotnicki, J., Ishido, T., Ueda, H., Hata, M., 2021. Hydrothermal and Magmatic System of a Volcanic Island Inferred From Magnetotellurics, Seismicity, Self-potential, and Thermal Image: An Example of Miyakejima (Japan). Journal of Geophysical Research: Solid Earth 126, e2021JB022034. https://doi.org/10.1029/2021JB022034Gresse, M., Vandemeulebrouck, J., Byrdina, S., Chiodini, G., Revil, A., Johnson, T.C., Ricci, T., Vilardo, G., Mangiacapra, A., Lebourg, T., Grangeon, J., Bascou, P., Metral, L., 2017. Three-Dimensional Electrical Resistivity Tomography of the Solfatara

Crater (Italy): Implication for the Multiphase Flow Structure of the Shallow Hydrothermal System. Journal of Geophysical Research: Solid Earth 122, 8749–8768. https://doi.org/10.1002/2017JB014389Gresse, M., Vandemeulebrouck, J., Byrdina, S., Chiodini, G., Roux, P., Rinaldi, A.P., Wathelet, M., Ricci, T., Letort, J., Petrillo, Z., Tuccimei, P., Lucchetti, C., Sciarra, A., 2018. Anatomy of a fumarolic system inferred from a multiphysics approach. Scientific Reports 2018 8:1 8, 1–11. https://doi.org/10.1038/s41598-018-25448-yGurioli, L., Zanella, E., Gioncada, A., Sbrana, A., 2012. The historic magmatic-hydrothermal eruption of the Breccia di Commenda, Vulcano, Italy. Bull Volcanol 74, 1235–1254. https://doi.org/10.1007/s00445-012-0590-4Hogg, C., Kiyan, D., Rath, V., Byrdina, S., Vandemeulebrouck, J., Revil, A., Viveiros, F., Carmo, R., Silva, C., Ferreira, T., 2018. 3-D interpretation of short-period magnetotelluric data at Furnas Volcano, Azores Islands. Geophysical Journal International 213, 371–386. https://doi.org/10.1093/gji/ggx512Inguaggiato, S., Vita, F., Diliberto, I.S., Mazot, A., Calderone, L., Mastrolia, A., Corrao, M., 2022. The Extensive Parameters as a Tool to Monitoring the Volcanic Activity: The Case Study of Vulcano Island (Italy). Remote Sensing 14, 1283. https://doi.org/10.3390/rs14051283INGV, 2022. Bollettini settimanali INGV Vulcano. Istituto Nazionale di Geofisica e Vulcanologia.Kelbert, A., Meqbel, N., Egbert, G.D., Tandon, K., 2014. ModEM: A modular system for inversion of electromagnetic geophysical data. Computers and Geosciences 66, 40–53. https://doi.org/10.1016/j.cageo.2014.01.010Keller, J., 1980. The island of Vulcano. REND. SOC. ITAL. MINERAL. PETROL.; ISSN 0037-8828; ITA; DA. 1980; VOL. 36; NO 1; PP. 369-414; H.T. 1; ABS. ITA; CART. GEOL.; ECH. 1:10 000.Meqbel, N.M.M., 2009. The electrical conductivity structure of the Dead Sea Basin derived from 2D and 3D inversion of magnetotelluric data (PhD Thesis).Paonita, A., Federico, C., Bonfanti, P., Capasso, G., Inguaggiato, S., Italiano, F., Madonia, P., Pecoraino, G., Sortino, F., 2013. The episodic and abrupt geochemical changes at La Fossa fumaroles (Vulcano Island, Italy) and related constraints on the dynamics, structure, and compositions of the magmatic system. Geochimica et Cosmochimica Acta 120, 158–178. https://doi.org/10.1016/j.gca.2013.06.015Paonita, A., INGV-PA Monitoring Team, INGV-OE Monitoring Team, 2022. The 2021- ongoing volcanic unrest at Vulcano island (Italy): clues from the INGV multidisciplinary surveillance network, in: Abstract Volume 5° Conferenza A. Ritmann, Catania 29 September 1st October 2022, Misc. INGV.Peccerillo, A., Frezzotti, M.L., De Astis, G., Ventura, G., 2006. Modeling the magma plumbing system of Vulcano (Aeolian Islands, Italy) by integrated fluid-inclusion geobarometry, petrology, and geophysics. Geology 34, 17–20. https://doi.org/10.1130/g22117.1Pous, J., Heise, W., Schnegg, P.A., Muoz, G., Martí, J., Soriano, C., 2002. Magnetotelluric study of the Las Canadas caldera (Tenerife, Canary Islands): Structural and hydrogeological implications. Earth and Planetary Science Letters 204, 249–263. https://doi.org/10.1016/S0012-821X(02)00956-1Revil, A., Finizola, A., Piscitelli, S., Rizzo, E., Ricci, T., Crespy, A., Angeletti, B., Balasco, M., Barde Cabusson, S., Bennati, L., Bolève, A., Byrdina, S., Carzaniga, N., Di Gangi, F., Morin, J., Perrone, A., Rossi, M., Roulleau, E., Suski, B., 2008. Inner structure of La Fossa di Vulcano (Vulcano Island, southern Tyrrhenian Sea, Italy) revealed by high-resolution electric resistivity tomography coupled with self-potential, temperature, and CO_2 diffuse degassing measurements. Journal of Geophysical Research 113, B07207. https://doi.org/10.1029/2007JB005394Revil, A., Johnson, T.C., Finizola, A., 2010. Three-dimensional resistivity tomography of Vulcan's forge, Vulcano Island, southern Italy: THREE-DIMENSIONAL RESISTIVITY TOMOGRAPHY OF VULCANO. Geophys. Res. Lett. 37, n/a-n/a. https://doi.org/10.1029/2010GL043983Rosi, M., Di Traglia, F., Pistolesi, M., Esposti Ongaro, T., de' Michieli Vitturi, M., Bonadonna, C., 2018. Dynamics of shallow hydrothermal eruptions: new insights from Vulcano's Breccia di Commenda eruption. Bull Volcanol 80, 83. https://doi.org/10.1007/s00445-018-1252-yRuch, J., Vezzoli, L., De Rosa, R., Di Lorenzo, R., Acocella, V., 2016. Magmatic control along a strike-slip volcanic arc: The central Aeolian arc (Italy): MAGMATISM AND STRIKE-SLIP FAULTING. Tectonics 35, 407–424. https://doi.org/10.1002/2015TC004060Seki, K., Kanda, W., Mannen, K., Takakura, S., Koyama, T., Noguchi, R., Yukutake, Y., Ishikawa, M., Fukai, M., Harada, M., Abe, Y., 2021. Imaging the Source Region of the 2015 Phreatic Eruption at Owakudani, Hakone Volcano, Japan, Using High-Density Audio-Frequency Magnetotellurics. Geophysical Research Letters 48, e2020GL091568. https://doi.org/10.1029/2020GL091568Seki, K., Kanda, W., Tanbo, T., Ohba, T., Ogawa, Y., Takakura, S., Nogami, K., Ushioda, M., Suzuki, A., Saito, Z., Matsunaga, Y., 2016. Resistivity structure and geochemistry of the Jigokudani Valley hydrothermal system, Mt. Tateyama, Japan. Journal of Volcanology and Geothermal Research 325, 15–26. https://doi.org/10.1016/j.jvolgeores.2016.06.010Selva, J., Acocella, V., Bisson, M., Caliro, S., Costa, A., Della Seta, M., De Martino, P., de Vita, S., Federico, C., Giordano, G., Martino, S., Cardaci, C., 2020. Multiple natural hazards at volcanic islands: a review for the Ischia volcano (Italy). Journal of Applied Volcanology. https://doi.org/10.1186/s13617-019-0086-4Soueid Ahmed, A., Revil, A., Byrdina, S., Coperey, A., Gailler, L., Grobbe, N., Viveiros, F., Silva, C., Jougnot, D., Ghorbani, A., Hogg, C., Kiyan, D., Rath, V., Heap, M.J., Grandis, H., Humaida, H., 2018. 3D electrical conductivity tomography of volcanoes. Journal of Volcanology and Geothermal Research 356, 243–263. https://doi.org/10.1016/j.jvolgeores.2018.03.017Troiano, A., Di Giuseppe, M.G., Patella, D., Troise, C., De Natale, G., 2014. Electromagnetic outline of the Solfatara-Pisciarelli hydrothermal system, Campi Flegrei (Southern Italy). Journal of Volcanology and Geothermal Research 277, 9–21. https://doi.org/10.1016/j.jvolgeores.2014.03.005Troiano, A., Isaia, R., Di Giuseppe, M.G., Tramparulo, F.D.A., Vitale, S., 2019. Deep Electrical Resistivity Tomography for a 3D picture of the most active sector of Campi Flegrei caldera. Scientific Reports 9. https://doi.org/10.1038/s41598-019-51568-0Troiano, A., Isaia, R., Tramparulo, F.D.A., Di Giuseppe, M.G., 2021. The Pisciarelli main fumarole mechanisms reconstructed by electrical resistivity and induced polarization imaging. Scientific Reports 11, 18639. https://doi.org/10.1038/S41598-021-97413-1Troiano, A., Petrillo, Z., Di Giuseppe, M.G., Balasco, M., Diaferia, I., Di Fiore, B., Siniscalchi, A., Patella, D., Troiano, A., Petrillo, Z., Giuseppe, M.G.D., Balasco, M., Diaferia, I., Fiore, B.D., Siniscalchi, A., Patella, D., 2008. About the shallow resistivity structure of Vesuvius volcano. Annals of Geophysics 51, 181–189. https://doi.org/10.4401/ag-3043Tsukamoto, K., Aizawa, K., Chiba, K., Kanda, W., Uyeshima, M., Koyama, T., Utsugi, M., Seki, K., Kishita, T., 2018. Three-Dimensional Resistivity Structure of Iwo-Yama Volcano, Kirishima Volcanic Complex, Japan: Relationship to Shallow Seismicity, Surface Uplift, and a Small Phreatic Eruption. Geophys. Res. Lett. 45. https://doi.org/10.1029/2018GL080202Unsworth, M., Rondenay, S., 2013. Mapping the distribution of fluids in the crust and lithospheric mantle utilizing geophysical methods, in: Lecture Notes in Earth System Sciences. https://doi.org/10.1007/978-3-642-28394-9_13Ventura, G., Vilardo, G., Milano, G., Pino, N.A., 1999. Relationships among crustal structure, volcanism and strike–slip tectonics in the Lipari–Vulcano Volcanic Complex (Aeolian Islands, Southern Tyrrhenian Sea, Italy). Physics of the Earth and Planetary Interiors 116, 31–52. https://doi.org/10.1016/S0031-9201(99)00117-XVilardo, G., Ventura, G., Sessa, E.B., Terranova, C., 2013. Morphometry of the Campi Flegrei caldera (Southern Italy). http://dx.doi.org/10.1080/17445647.2013.842508 9, 635–640. https://doi.org/10.1080/17445647.2013.842508Yang, J., Min, D.-J., Yoo, H.-S., 2010. Sea effect correction in magnetotelluric (MT) data and its application to MT soundings carried out in Jeju Island, Korea: Sea effect correction in MT data. Geophysical Journal International 182, 727–740. https://doi.org/10.1111/j.1365-246X.2010.04676.x